

Effect of carrier mobility on performance of perovskite solar cells

Yi-Fan Gu(顾一帆), Hui-Jing Du(杜会静), Nan-Nan Li(李楠楠), Lei Yang(杨蕾), Chun-Yu Zhou(周春宇)

Citation: Chin. Phys. B . 2019, 28(4): 048802. **doi:** 10.1088/1674-1056/28/4/048802
Journal homepage: http://cpb.iphy.ac.cn; http://iopscience.iop.org/cpb

What follows is a list of articles you may be interested in

Promise of commercialization: Carbon materials for low-cost perovskite solar cells

Yu Cai(蔡宇), Lusheng Liang(梁禄生), Peng Gao(高鹏)

Chin. Phys. B . 2018, 27(1): 018805. **doi:** 10.1088/1674-1056/27/1/018805

Efficient design of perovskite solar cell using mixed halide and copper oxide

Navneet kour, Rajesh Mehra, Chandni

Chin. Phys. B . 2018, 27(1): 018801. **doi:** 10.1088/1674-1056/27/1/018801

O_3 fast and simple treatment-enhanced p-doped in Spiro-MeOTAD for CH_3NH_3I vapor-assisted processed $CH_3NH_3PbI_3$ perovskite solar cells

En-Dong Jia(贾恩东), Xi Lou(娄茜), Chun-Lan Zhou(周春兰), Wei-Chang Hao(郝维昌), Wen-Jing Wang(王文静)

Chin. Phys. B . 2017, 26(6): 068803. **doi:** 10.1088/1674-1056/26/6/068803

Simulation design of P-I-N-type all-perovskite solar cells with high efficiency

Hui-Jing Du(杜会静), Wei-Chao Wang(王韦超), Yi-Fan Gu(顾一帆)

Chin. Phys. B . 2017, 26(2): 028803. **doi:** 10.1088/1674-1056/26/2/028803

Device simulation of lead-free $CH_3NH_3SnI_3$ perovskite solar cells with high efficiency

Hui-Jing Du(杜会静), Wei-Chao Wang(王韦超), Jian-Zhuo Zhu(朱键卓)

Chin. Phys. B . 2016, 25(10): 108802. **doi:** 10.1088/1674-1056/25/10/108802

Effect of carrier mobility on performance of perovskite solar cells*

Yi-Fan Gu(顾一帆), Hui-Jing Du(杜会静)†, Nan-Nan Li(李楠楠), Lei Yang(杨蕾), and Chun-Yu Zhou(周春宇)‡

Key Laboratory for Microstructural Material Physics of Hebei Province, School of Science, Yanshan University, Qinhuangdao 066004, *China*

(Received 7 November 2018; revised manuscript received 31 January 2019; published online 5 March 2019)

The high carrier mobility and long diffusion length of perovskite material have been regarded because of its excellent photovoltaic performance. However, many studies have shown that a diffusion length longer than 1 μm and higher carrier mobility have no positive effect on the cells' performance. Studies of organic solar cells have demonstrated the existence of an optimal mobility value, while systematic research of the carrier mobility in the PSCs is very rare. To make these questions clear, the effect of carrier mobility on perovskite solar cells' performance is studied in depth in this paper by simulation. Our study shows that the optimal mobility value of the charge transportation layer and absorption layer are influenced by both doping concentration and layer thickness. The appropriate carrier mobility can reduce the carrier recombination rate and enhance the carrier concentration, thus improving the cells' performance. A high efficiency of 27.39% is obtained in the simulated cell with the combination of the optimized parameters in the paper.

Keywords: perovskite solar cells, device simulation, carrier mobility, photovoltaic performance

PACS: 88.40.H–, 88.40.hj, 88.40.fc **DOI:** 10.1088/1674-1056/28/4/048802

1. Introduction

Perovskite solar cells (PSCs) have attracted considerable attention in the past few years due to their rapid photovoltaic efficiency improvement, from 10% in 2012[1,2] to 23.2% in 2018.[3] The excellent photovoltaic performance of PSCs is ascribed to its excellent optoelectrical characteristics, such as high light absorption coefficient,[4,5] long carrier diffusion length,[6,7] high carrier mobility,[8,9] and long recombination lifetime.[9] The transportation of carriers from the absorber to charge transport layer and the collection of them by electrodes are key processes to determine the cell efficiency, hence carrier mobility is one of the significant factors affecting cell performance. The carrier mobility and diffusion length of perovskite crystal have reached to hundreds of $cm^2/V{\cdot}s$ and hundreds of μm respectively. However, can the higher mobility and the longer diffusion length lead to better PSCs' performance? Research has drawn different conclusions about the influence of carrier mobility[10–12] and diffusion length[10,13–15] on PSCs performance. Simulation studies based on one-dimensional simulation software SCAPS show that the diffusion length longer than 1 μm and higher mobility of the carriers have no positive effect on the cell performance promotion,[13,15] and high mobility of the charge transport layer is also necessary for the high efficiency.[16,17] The influence of carrier mobility on the cell performance is restricted by other cell parameters, such as doping concentration, layer thickness, *etc*. In these papers, these factors were not considered as a whole. Carrier transportation can be enhanced if the parameters of the cell are well matched, and thus improve cell performance. Many experimental and theoretical studies of the mobility influence on the organic solar cells' performance demonstrated that there exists an optimal value of mobility for obtaining high efficiency organic cells.[18–21] While the systematic study of carrier mobility in PSCs is very rare, this would affect the best utilization of the excellent carriers' transportation characters of perovskite material to improve cell performance. To clarify these questions, we construct the device model and simulate the carrier transportation to understand the mechanism of carrier mobility influencing the cell performance. Our simulation study shows that the optimal mobility also exists in perovskite solar cells, and by matching the carrier mobility of the transportation layer and the absorption layer, the efficiency of perovskite solar cells can be enhanced. The optimized cells' structure with a diffusion length of nearly 1.9 μm and the photovoltaic efficiency of 27.39% is obtained ultimately.

2. Device model and simulation parameters

In our previous research on lead-free perovskite solar cells,[22] we obtained an efficiency of 23.36% by optimizing the doping concentration, defect density and electron affinity of the buffer. To elucidate the mechanism of high carrier mobility and long diffusion length of the perovskite materials influencing the cell performance, our simulation is based on that previous optimized structure (glass substrate/TCO/buffer layer TiO_2 (ETM)/absorption layer $CH_3NH_3SnI_3$/hole transport material (HTM) spiro-OMeTAD/metal back contact) to

*Project supported by the National Natural Science Foundation of China (Grant No. 61704147) and the Science Fund from the Education Department of Hebei Province, China (Grant No. QN2017150).

†Corresponding author. E-mail: Hjdu@ysu.edu.cn

‡Corresponding author. E-mail: zhouchunyu@ysu.edu.cn

© 2019 Chinese Physical Society and IOP Publishing Ltd

avoid the influence of other cell parameters. The parameters of that previous structure, serving as our initial simulation parameters, are listed in the following Table 1. The simulation principle, the cell architecture, and other simulation parameters selected for each layer can also be found from our previous studies.[22]

Table 1. Simulation parameters and performances of device during optimization. The parameters in bold text are the optimal value during the optimization.

	Parameters of the ETM, absorber, and HTM			Performance of the device			
	Thickness/nm	Mobility/(cm^2/V·s)	Doping concentration/cm^{-3}	V_{oc}/V	J_{sc}/(mA/cm^2)	*FF*/%	*PCE*/%
Initial cell	30, 600, 200	20/10, 1.6/1.6, $2\times10^{-4}/2\times10^{-4}$	1×10^{16}, 1.3×10^{16}, 2×10^{19}	0.92	31.59	79.99	23.36
1st optimization absorber	30, 1100 (vari.), 200	20/10, 5/5 (vari.), $2\times10^{-4}/2\times10^{-4}$	1×10^{16}, 8×10^{15} (vari.), 2×10^{19}	0.90	33.30	82.38	24.78
Optimization HTM	30, 1100, 5 (vari.)	20/10, 5/5, 0.1/0.1 (vari.)	1×10^{16}, 8×10^{15}, 3×10^{19} (vari.)	0.90	33.32	82.66	24.89
Optimization ETM	5 (vari.), 1100, 5	20/10 (vari.), 5/5, 0.1/0.1	3×10^{19} (vari.), 8×10^{15}, 3×10^{19}	0.95	34.16	83.95	27.17
2nd optimization absorber	5, 1200 (vari.), 5	20/10, 12/12 (vari.), 0.1/0.1	3×10^{19}, 1.2×10^{16} (vari.), 3×10^{19}	0.94	34.21	84.97	27.39

The current density–voltage (*J*–*V*) characteristic curve of the cell with initial parameters is shown in Fig. 1 (curve 1). Short-circuit current density (J_{sc}) of 31.59 mA/cm^2, open-circuit voltage (V_{oc}) of 0.92 V, fill factor (*FF*) of 79.99%, and power conversion efficiency (*PCE*) of 23.36% are obtained.

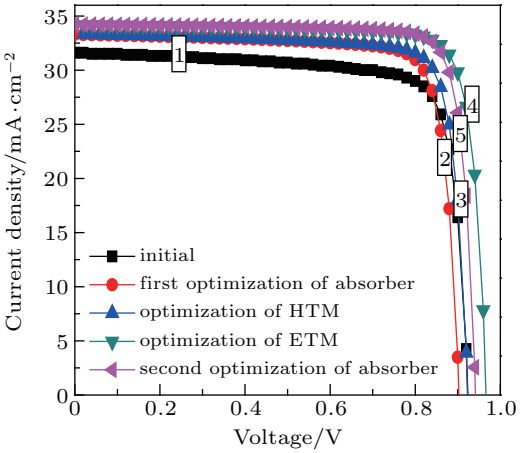


Fig. 1. *J*–*V* curves of PSCs during optimization.

Based on previous optimized structure, we further investigate the relation between the carrier mobility and the cell performance. Taking into account the influence of each layer on the performance of perovskite solar cells, the optimization process consists of four steps. The parameters of thickness, carrier mobility, and doping concentration are optimized in the absorber layer, HTM, and ETM layers in sequence at the first three steps. At the fourth step, the parameters of the absorber layer are re-optimized to realize the matching optimization of all the parameters. Experimental research has shown that the mobility μ is independent of charge carrier concentration of the perovskite absorber layer at lower concentrations (10^{16} cm^{-3}–10^{18} cm^{-3}).[23,24]

3. Results and discussion

3.1. Optimization of the absorption layer

In this step, the relation of the mobility with the thickness and doping concentration of the absorber is investigated first based on the parameters of the initial cell in Table 1. Figures 2 and 3 illustrate the effects of mobility on the device performance under various absorber thickness values and doping concentrations. It can be seen that the optimal value of mobility (Figs. 2(a) and 3(a)) changes with the absorber thickness and doping concentration. At an optimal value of 5 cm^2/V·s (1100 nm), the cell efficiency increases slightly from the initial 23.36% to 24.66%. With the enhancement of the mobility, the *FF* and the J_{sc} increase significantly, which is consistent with the experimental research in the literature.[19,25] When the carrier mobility μ is smaller than 10 cm^2/V·s, efficiency and J_{sc} of the device first rise and then decreases with thickness increasing, and a moderate thickness of 800 nm is conducible to the improvement of efficiency, so we adopted an optimal thickness 600 nm of the absorption layer when μ was 2 cm^2/V·s in our previous paper.[22] This is consistent with the experimental research that the absorber thickness is always about 700 nm, because the mobility of the polycrystalline perovskite film is always lower than 10 cm^2/V·s.[3,26,27] When μ is higher than 10 cm^2/V·s, the absorber thicker than 800 nm is more suitable to the obtaining of a higher efficiency, which is embodied with the significant increment of J_{sc}. The higher the thickness absorber layer, the more the generated photo-carriers is, and especially more longwaves can be absorbed.[28,29] This can be seen in the external quantum efficiency (*QE*) curve (Fig. 4), where the *QE* at the longwave increases with the augmentation of the absorber thickness.

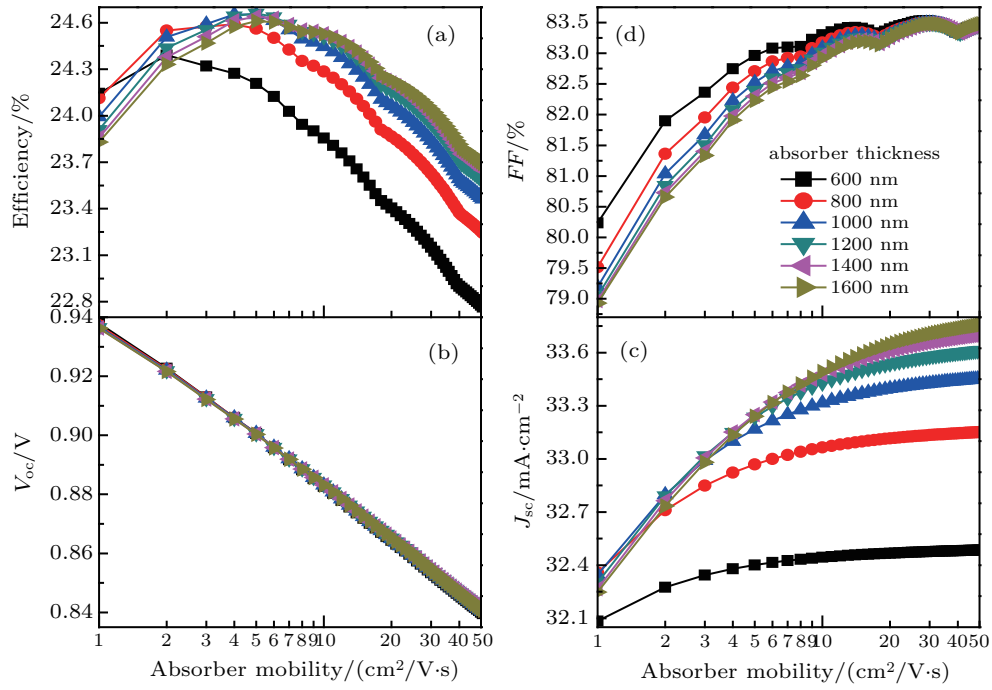


Fig. 2. Variations of (a) efficiency, (b) V_{oc}, (c) J_{sc}, and (d) FF of PSCs with thickness and mobility of the first optimization of absorber.

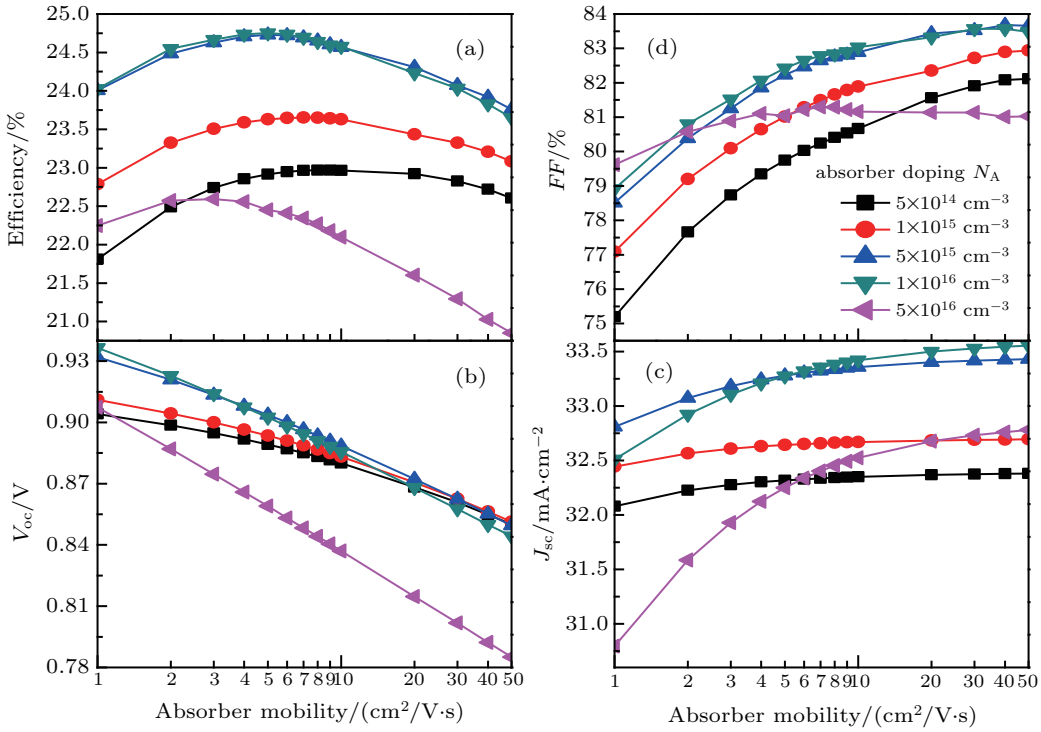


Fig. 3. Variations of (a) efficiency, (b) V_{oc}, (c) J_{sc}, and (d) FF of PSCs with doping concentration and mobility of the first optimization of absorber.

Figure 3 illustrates the effects of mobility on the cell performance at various doping concentrations of the absorber layer based on the optimized absorber thickness of 800 nm obtained from Fig. 2. The J_{sc} and FF both increase with mobility increasing at different doping concentrations, especially the J_{sc} can be significantly augmented (Fig. 3(c)). The obvious influence of mobility on J_{sc} can be observed when N_A is higher than 1×10^{16} cm^{-3}. With a certain mobility, say, $\mu = 6$ cm^2/V·s, J_{sc} first increases with the augment of doping concentration and then decreases significantly with N_A further increasing to 5×10^{16} cm^{-3}. This is because both J_{sc} and recombination rate increase with the augment of doping concentration. Mobility can surmount the contradiction between high J_{sc} and high recombination rate caused by the

high doping concentration. Recombination can be weakened through good transportation performance of perovskite material with high mobility, which would be explained in the paper in the last simulation step (see Fig. 11). The optimal value of mobility gradually decreases with N_A increasing, thus lowering the negative effect of the doping concentration increment (see Fig. 3(a)). Moderate doping concentration (5×10^{15} cm$^{-3} \leq N_A < 1\times10^{16}$ cm^{-3}) is beneficial to the improvement of efficiency for $\mu > 10$ cm^2/V·s.

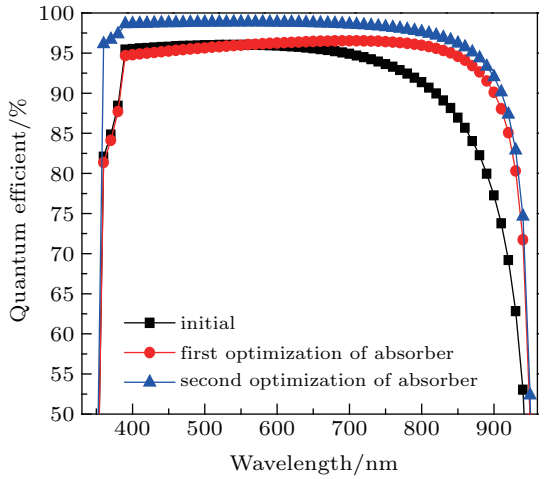


Fig. 4. Curves of external quantum efficiency *versus* wavelength of PSCs during optimization.

This analysis presents that monotonically increasing the mobility of the absorber layer is not beneficial to the performance of the PSCs. Taking into account the influence of the thickness and doping concentration, an optimal value of mobility exists. The corresponding $\boldsymbol{J}$–V characteristic curve (curve 2) is shown in Fig. 1, and $\boldsymbol{J}_{sc}$ rises significantly from the initial 31.59 mA/cm^2 to 33.30 mA/cm^2. The V_{oc} of 0.90 V, FF of 82.38%, and PCE of 24.78% are obtained at this preliminary optimization of the absorption layer.

The transportation parameter's matching between the absorber and the charge transport layer is important to avoid the excessive accumulation of the carriers at their interface during the photon-generated carriers transporting to the corresponding electrodes. Hence, after the absorber layer optimization, the carrier mobility and other parameters, such as doping concentration and thickness, of HTM and ETM should also be optimized.

3.2. Optimization of the charge transport layer

3.2.1. Optimization of the hole transport layer (HTM)

The HTM layer is optimized based on the preliminarily optimized absorber layer. The effects of mobility on the performance of perovskite solar cells under various HTM thickness values (Fig. 5(a)) and doping concentrations (Fig. 5(b)) are given. In a 3-nm–15-nm range of HTM thickness, when the mobility of HTM increases from 10^{-4} cm^2/V·s to 5×10^{-2} cm^2/V·s, the efficiency of perovskite solar cells increases gradually. Little change of the efficiency can be seen for $\mu > 1\times10^{-2}$ cm^2/V·s because the carriers' diffusion length is longer than the thickness of the HTM. When doping concentration is smaller than 1×10^{19} cm^{-3}, PSCs' efficiency augments gradually with mobility increasing and reaches a saturation level at an HTM mobility of 0.1 cm^2/V·s. When the doping concentration is 1×10^{19} cm^{-3}, the effect of the mobility is very weak on the cell's efficiency.

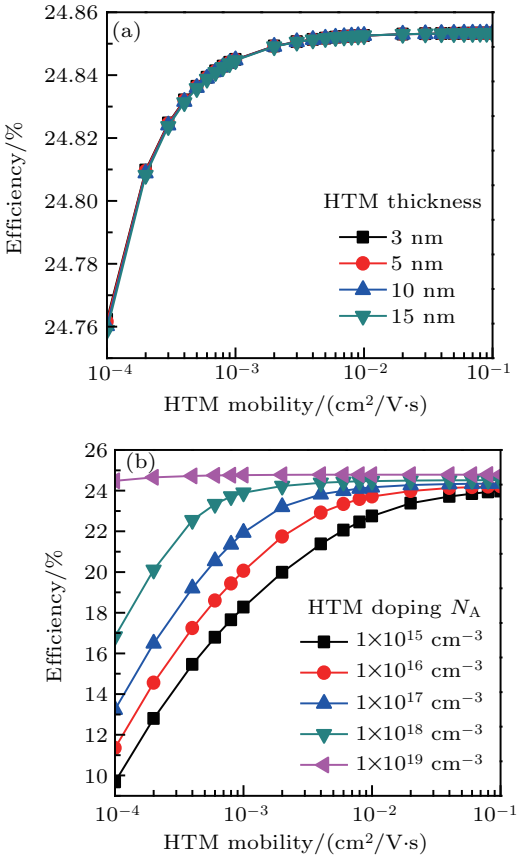


Fig. 5. Plots of efficiency *versus* mobility of PSCs for various (a) thickness values and (b) doping concentrations of HTM.

Figure 6 shows the variation trends of device performance affected by thickness, doping concentration, and mobility of HTM, respectively. During simulation, other two parameters are kept unchanged when the optimized parameters are extracted from Fig. 5 with an HTM thickness of 5 nm, a doping concentration of 1×10^{19} cm^{-3} and mobility of 0.1 cm^2/V·s. The efficiency, $\boldsymbol{J}_{sc}$ and FF rise with the mobility of HTM increasing, and the open-circuit voltage V_{oc} is almost constant, which is in accordance with the work of Alnuaimi.[30] Doping concentration enhancement of HTM can increase its conductivity, hole mobility and charge density, and this will significantly improve the device performance.[31,32] The improvement of device performance with doping concentration growing is consistent with the scenario in the literature,[33] and we set 3×10^{19} cm^{-3} and 0.1 cm^2/V·s as the optimal doping concentration and mobility of HTM, respectively. The optimal

mobility value of 0.1 $cm^2/V{\cdot}s$ is in agreement with that in the literature.[30] Although thinner thickness is more beneficial to the cell performance promoting, considering the difficulty of preparation, the optimal thickness value of HTM is taken to be 5 nm. After the optimization of the HTM, a *PCE* of 24.89% is obtained with $\boldsymbol{J}_{sc}$ of 33.32 mA/cm^2, V_{oc} of 0.904 V, FF of 82.66%, and its $\boldsymbol{J}$–V curve is depicted with curve 3 in Fig. 1. In comparison with the preliminary optimization of the absorber layer (curve 2 Fig. 1), an obvious augment of V_{oc} is obtained.

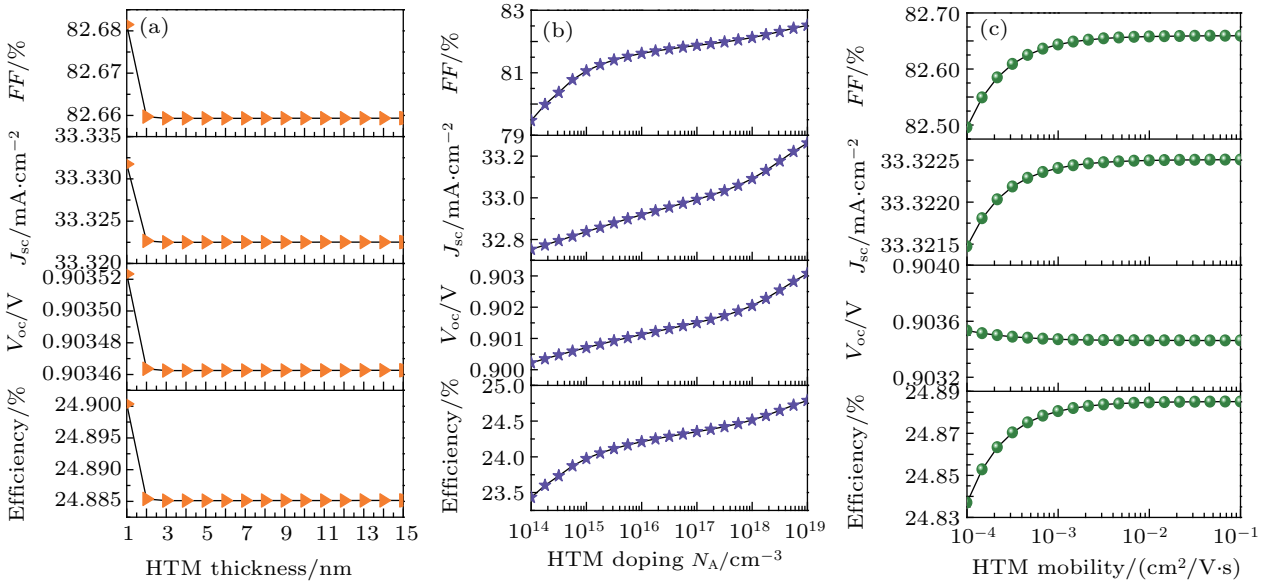


Fig. 6. Variations of performance parameters of PSCs with (a) thickness, (b) doping concentration, and (c) mobility of HTM.

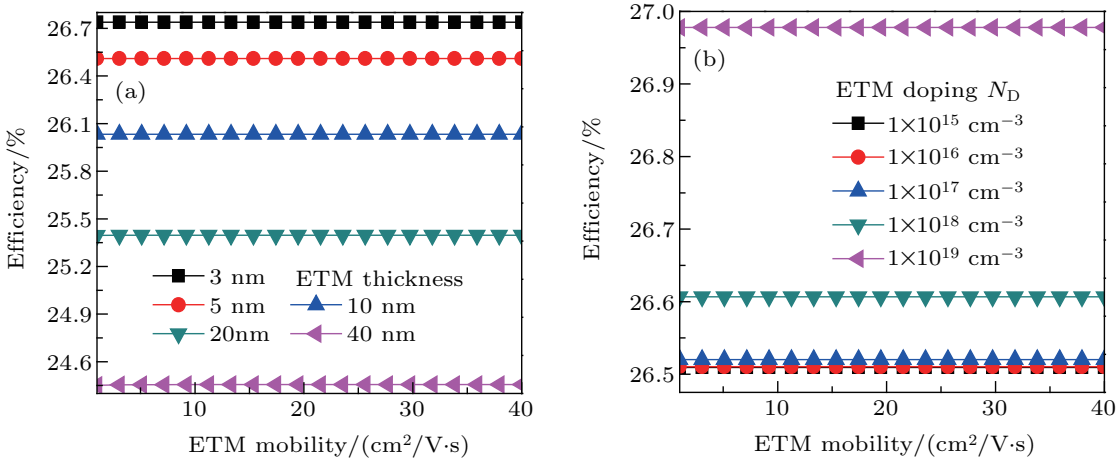


Fig. 7. Plots of efficiency of PSC *versus* mobility for (a) various thickness values and (b) various doping concentrations of ETM.

3.2.2. Optimization of the electron transport layer (ETM)

The parameters of the ETM layer are optimized in sequence. Figure 7 reveals the influences of ETM mobility on device efficiency with various thickness values and doping concentrations. The efficiency decreases with the thickness of ETM increasing from 3 nm to 20 nm but does not vary with the mobility of ETM. Figure 8 exhibits the variations in thickness, doping concentration, and mobility of ETM *versus* device performance parameters, respectively. When the ETM thickness increases from 1 nm to 15 nm, all the performance parameters, such as $\boldsymbol{J}_{sc}$, V_{oc}, FF, and *PCE* of the device first rise and then decrease, and there exists an optimal thickness value of 5 nm for the ETM layer. For polycrystalline perovskite, $CH_3NH_3PbI_3$, whose diffusion length is short, a thick mesoporous ETM layer is generally required.[34] But for the single crystal perovskite with L on the order of micros, the ETM layer is not necessary for the high efficiency cell. The TiO_2 ETM of the planner structured PSC can be prepared fast by spraying pyrolysis with good crystallinity.[35]

The device performance parameters continuously increase as the doping concentration of ETM increases because of the enhancement of the carrier concentration and conductivity,[36,37] while they do not vary with the mobility of optimization of electron transport layer. We take 3×10^{19} cm^{-3} as the optimum doping concentration for ETM, which is compatible to that in

Refs. [38] and [39] and highly efficient semiconducting TiO_2 can also be obtained by aerosol pyrolysis.[40] The importance of the high doping of the TiO_2 ETM to match the HTM with high mobility was also investigated systematically in Ref. [17]. The J–V curve of the device after the optimization of ETM is illustrated in curve 4 of Fig. 1, and J_{sc} of 34.16 mA/cm^2, V_{oc} of 0.947 V, FF of 83.95%, and PCE of 27.17% are obtained.

Because the diffusion length L of micrometer magnitude caused by the high mobility (1 cm^2/V·s–40 cm^2/V·s) of ETM is far beyond the ETM thickness (5 nm–40 nm), the influence of the ETM mobility on device performance is weaker than that of the HTM.

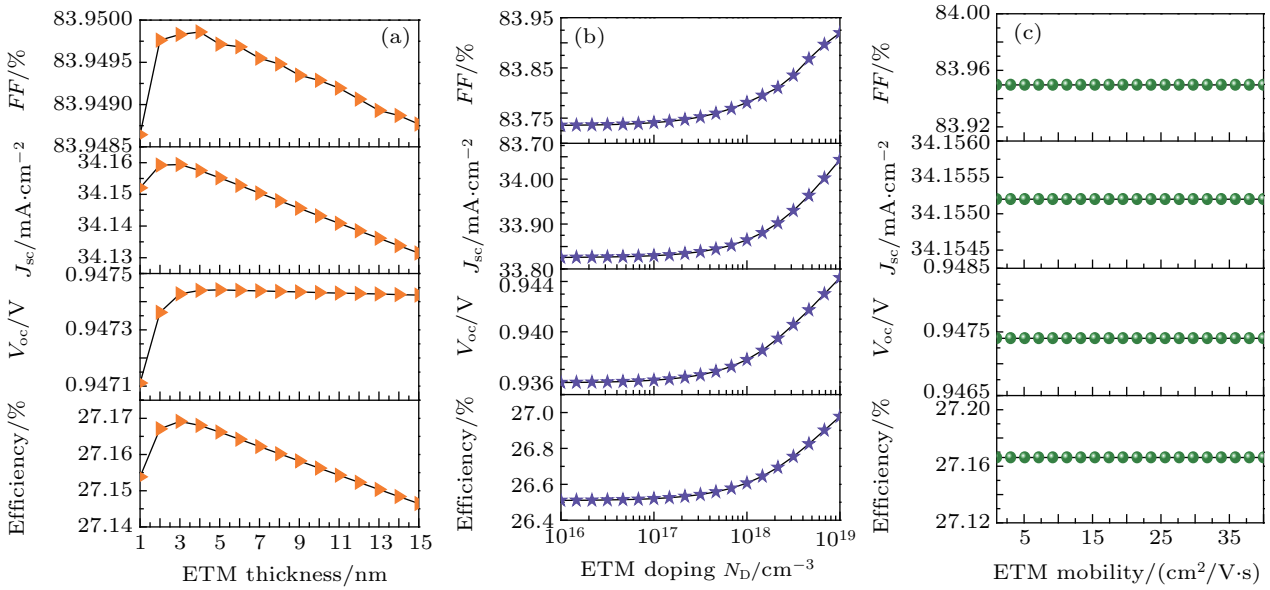


Fig. 8. Variations of performance parameters of PSCs with (a) thickness, (b) doping concentration, and (c) mobility of ETM.

3.3. Ultimate optimization of absorption layer

After the preliminary optimization of the absorber and charge transport layer, ultimate optimization of the absorption layer is carried out to access a good match between layers. Figure 9 depicts the relationships between mobility and efficiency of PSCs at diverse thickness values and doping concentrations of the absorber layer. The optimal absorber thickness increases from about 800 nm to 1200 nm when μ rises from 3 cm^2/V·s to 12 cm^2/V·s, which can be seen from the partially detailed map inset in Fig. 9(a) clearly. A similar parabola relation between the absorber mobility and the cell efficiency is exhibited in an organic cell.[18,19] The optimal mobility is small for the thin absorber, and when the mobility of the absorber is higher than 10 cm^2/V·s, a thicker absorber is more beneficial to the cell efficiency improvement. This enhancement of the optimal thickness of the absorber is induced by increasing the absorber mobility and the $N_{A,D}$ of the charge transportation layer, the same change trend is observed in Ref. [41].

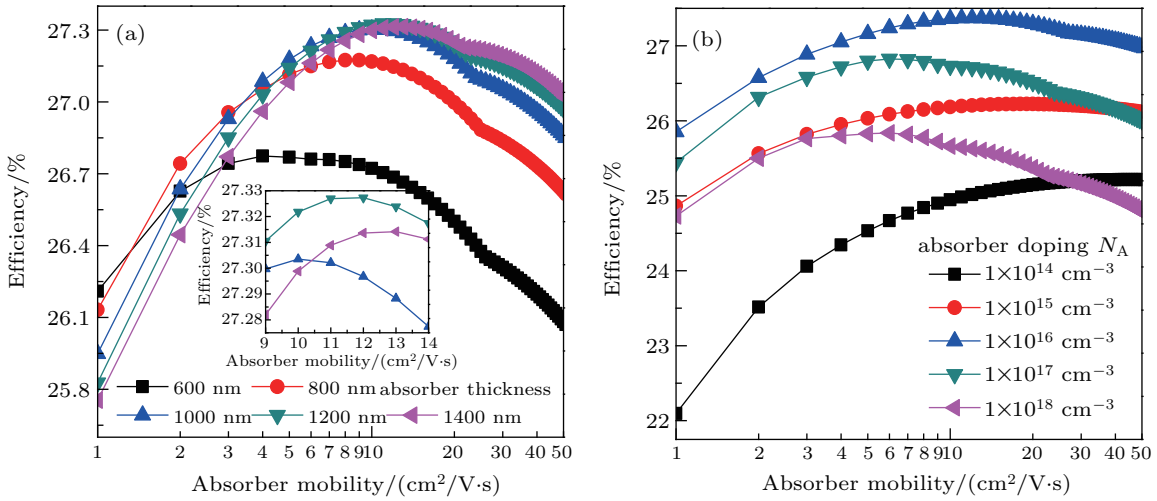


Fig. 9. Efficiency of PSCs as a function of mobility with (a) thickness and (b) doping concentration of the second optimization of absorber.

However, the excessive thickness and mobility do not achieve higher efficiency (Figs. 10(a) and 10(c)), and the efficiency reaches a saturation level at a thickness of 1200 nm. An optimal value of 12 cm^2/V·s for the mobility exists with an absorber thickness of 1200 nm.[42] When the doping concentration changes from 10^{14} cm^{-3} to 10^{16} cm^{-3}, the maximum efficiency of the cell appears at N_A of 1.2×10^{16} cm^{-3}. The enhancement of the mobility results in the increase of FF and J_{sc}, while the V_{oc} reduces. The V_{oc} augments obviously with N_A further increasing from 8×10^{15} cm^{-3} (preliminary optimization) to 1.2×10^{16} cm^{-3} (ultimate optimization), which is reflected in the J–V curves 2 and 4 in Fig. 1, respectively. The change of the optimal value of N_A is caused by increasing the optimal value of the thickness and mobility of the absorber.

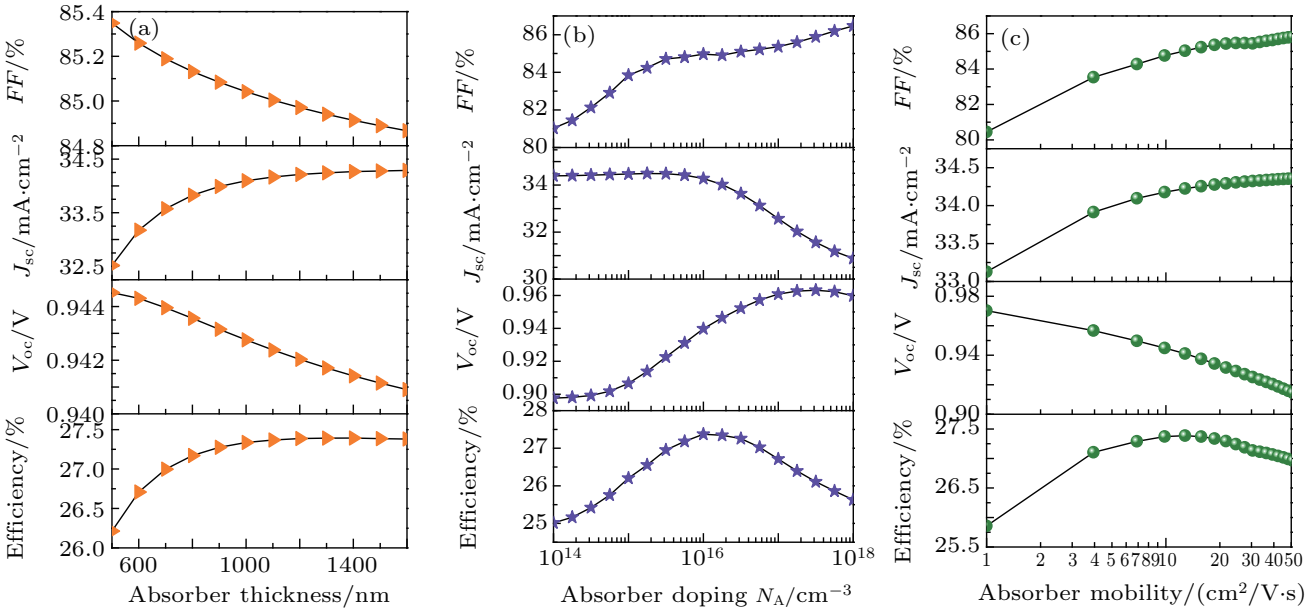


Fig. 10. Plots of PSCs' performance with (a) thickness, (b) doping concentration, and (c) mobility of the second optimization of absorber.

Finally, after the four optimizing steps, the device PCE reaches 27.39% with J_{sc} of 34.21 mA/cm^2, V_{oc} of 0.942 V, FF of 84.97%. The efficiency increases by 4.03% compared with the initial one, and this efficiency is highest, to our knowledge, for the single junction PSCs obtained by simulation. The optimal match between the mobility and other parameters of the absorber and the charge transport layer induces the value of J_{sc} and V_{oc} to obviously augment, which can be seen in the J–V characteristic curve (curve 5) of the ultimate optimized cell in Fig. 1.

4. Detailed analysis of the influence mechanism of carrier mobility on cell influence

4.1. Effect of mobility on J_{sc}

J_{sc} can be approximated as

$$J_{sc} = qG\left(L_n + w + L_p\right). \tag{1}$$

The photo-generation rate G can be considered as a constant under certain lighting conditions AM1.5. Depletion width w of the p-n junction depends on carrier concentration. The value of J_{sc} would ascend with the increase of diffusion length L, because the value of w is unchangeable in the $N_{A,D}$ invariable situation (Fig. 3(c)). The significant increase of J_{sc} as $N_{A,D}$ increases can be seen in Figs. 3(c), 6, and 8. This happens because the depletion width decreases due to the increase of $N_{A,D}$, and this can lower the contact resistance of the interface, which is favorable to the transportation of the carriers.

4.2. Effect of mobility on open-circuit voltage V_{oc}

Obvious improvement of V_{oc} is obtained for the optimized cell, and this is the combined influence of doping concentration and the carrier mobility. The formula of V_{oc} and reverse saturation current J_0 can be expressed as

$$V_{oc} = \ln\left(\frac{J_{sc}}{J_0}+1\right)\frac{k_BT}{q}, \tag{2}$$

$$J_0 = q\left(\frac{D_n n_i^2}{L_n N_A}+\frac{D_p n_i^2}{L_p N_D}\right). \tag{3}$$

According to the Einstein relationship and the diffusion length (L_n) formula, J can be described as

$$J_0 = q\left(\frac{\sqrt{\mu_n} n_i^2}{\sqrt{\tau} N_A}+\frac{\sqrt{\mu_p} n_i^2}{\sqrt{\tau} N_D}\right). \tag{4}$$

In our simulation, the lifetime τ can be considered as a constant in the case of invariable defect concentration. The value of J_0 decreases with the increase of $N_{A,D}$ of the charge transport layer. Owing to the influence of the strong increase of J_{sc} with the increase of $N_{A,D}$, the V_{oc} will increase based on

formula (2). Because of the considerable difference in magnitude between $N_{A,D}$ and $\mu_{n,p}$, the influence of mobility on J_0 is negligible.

According to formulas (1)–(4), V_{oc} can be expressed as

$$V_{oc} = \ln\left(\frac{G(2+w/L)}{\frac{n_i^2}{\tau N_A}+\frac{n_i^2}{\tau N_D}}\right)\frac{k_B T}{q}. \tag{5}$$

Keeping the $N_{A,D}$ constant, V_{oc} decreases with the enhancement of diffusion length, that is, V_{oc} decreases with the enhancement of mobility under the $N_{A,D}$ invariable condition (see Fig. 3(b)).

4.3. Effect of mobility on other cell parameters

The final part of this article is dedicated to investigating the contribution of mobility to recombination rate R, carrier density distribution, and band structure in planar heterojunction PSCs. The recombination rate of the process of optimization of ETM layer and the second optimization of the absorber layer is depicted in Fig. 11. The increasing of doping concentration of the absorber layer from 8×10^{15} cm^{-3} to 1.2×10^{16} cm^{-3} in the last optimization step should cause the recombination rate to increase, while a weakened recombination rate can be seen in Fig. 11.

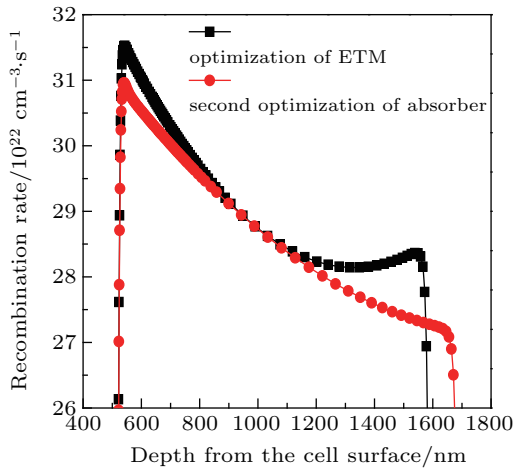


Fig. 11. Recombination distributions of different optimizations.

We ascribe the weakening of recombination to the increasing of mobility of the absorber from 5 cm^2/V·s to 12 cm^2/V·s, which improves the transportation performance of the cell. The influence of carrier mobility on the carrier transportation is studied based on the last optimized cell structure through the observation of carrier concentration distribution in the absorber layer with the mobility increasing from 2 cm^2/V·s to 40 cm^2/V·s (see Fig. 12). The empty and the solid symbols represent holes and electrons, respectively. The simulation is conducted based on the final optimization step, with keeping all the parameters constant, except for the enhanced mobility of the absorber. The carriers' concentration of the absorber does not rise consistently with the mobility increase, and the maximum concentration of carriers appears at a mobility of 12 cm^2/V·s, which is the optimal value of the mobility in the absorber. The enhanced drift velocity $\boldsymbol{v}$ ($v=\mu E$) of the carriers, caused by the improved mobility, can augment the concentration of carriers crossing the cell section, which benefits the cell performance improvement. While the enhanced carrier concentration also increases the recombination rate, and there is a competing mechanism between the improvement of the carrier transportation and the enhanced recombination brought by the enhanced mobility, only an optimal mobility value can improve the cell performance.[43]

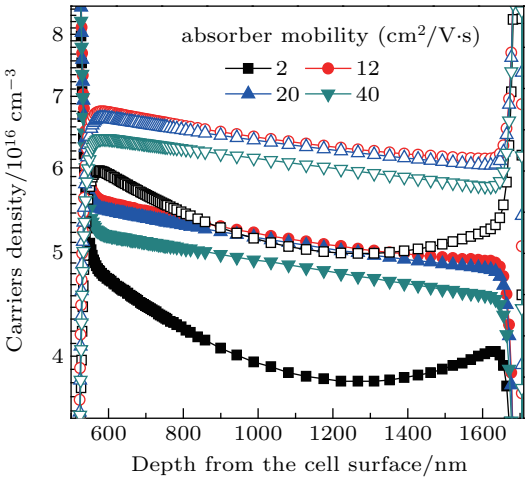


Fig. 12. Carrier's density distribution with different mobility values of absorber layer.

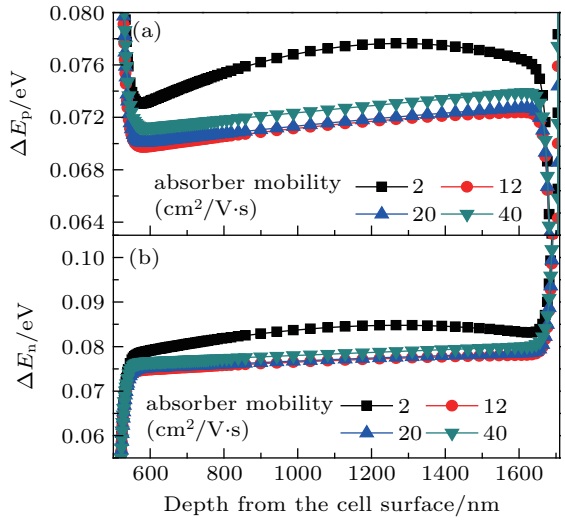


Fig. 13. Difference in quasi-Fermi energy (a) ΔE_p and (b) ΔE_n *versus* depth from cell surface for different mobility values of absorber layer.

The distribution of carriers in a nonequilibrium state is related to quasi-Femi energy. The energy bands of the simulated structure with different absorber mobility values are studied based on the last optimized cell structure, and we obtain the

energy difference between the E_v (E_c) and E_{Fp} (E_{Fn}) (Fig. 13). When the energy difference ΔE_p (ΔE_n) is smaller, the carrier concentration is higher. It can be seen that the electrons (holes) transport from the absorber layer to the ETM (HTM) layer, because of the rapid reduction of the ΔE_n (ΔE_p) at their interface. The fastest decline in ΔE, namely the fastest growing of the carrier concentration, appears at the architecture with a mobility of 12 $cm^2/V{\cdot}s$, which means the fastest transportation of the carriers. So the mobility of 12 $cm^2/V{\cdot}s$ is an optimal value of our simulated structure with the highest efficiency of 27.39%.

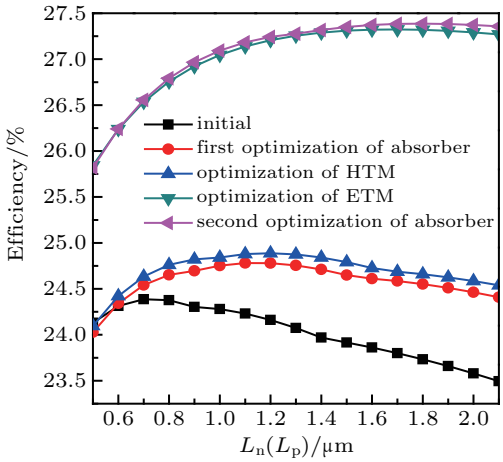


Fig. 14. Plots of efficiency of PSC *versus* carrier diffusion length L during optimization.

4.4. How long carrier diffusion length is enough to achieve high cell efficiency?

Getting a long diffusion length by improving perovskite process can enhance cell efficiency.[16] Diffusion length L of single $CH_3NH_3PbI_3$ crystal has reached 175 μm.[44] Now, a question arises: can the longer L achieve the better performance of the PSCs? In this paper, L is adjusted by changing the mobility, with the defect concentration of the absorber unchanged. The efficiency of the cell with the changing of L at the different optimization steps in the paper is shown in Fig. 14. The length L of 0.7 μm is enough to construct the initial cell with a small absorber thickness (600 nm), and this thickness value is consistent with those for most of the PSCs with high efficiency in the experimental research. The appropriate L rises with the increase of thickness and mobility of the absorber.[38] Finally, the highest efficiency appears at L of 1.9 μm, which is larger than the absorber thickness of 1200 nm. Many researchers have pointed out that L of 1 μm is enough to construct the cell device, but this conclusion is obtained under specified circumstances, such as the thickness of the absorber is about hundreds of nanometers. In Ref. [6], L (1.2 μm) is twice the $CH_3NH_3PbI_{3-x}Cl_x$ absorber thickness (500 nm). The L higher than the absorber thickness in the perovskite is needed for efficient carriers' extraction before significant recombination occurs. The J_{sc} is limited by the material's long wavelength response, and the higher absorber thickness benefits the strong red spectral absorption.[28,43] In Fig. 2, the trends of J_{sc}, and V_{oc} varying with absorber thickness are opposite, which can be seen as $\mu > 10$ $cm^2/V{\cdot}s$. Improving L (namely, mobility) of the perovskite material can avoid the joint reduction of J_{sc} and V_{oc} when the absorber layer thickness increases.

Many researchers have indicated that the *PCE* of the PSCs is insensitive to the absorber thickness beyond 600 nm, this lies in the fact that the recombination rate of the thicker perovskite layer is higher than that of the thinner layer. In the research by Jeon *et al.*,[3] the PSC reached a high efficiency of 23.2%. The absorber thickness is selected to be 600 nm to avoid the carriers crossing the grain boundaries during transporting to the electrodes. We expect that if the crystal size presented in Joen *et al.*'s research[3] can be improved to 1 μm and an absorber thicker than 600 nm can be obtained, the cell efficiency can be further improved based on our simulation. Now the single perovskite crystal with a size of 300 μm has been achieved in experiment.[44] High-performance PSC with absorber layer thickness of 1150 nm has been realized by the hot casting method.[42] And more importantly, the thick-film PSC has good stability. This research bodes well for the great potential of thick-film PSCs in mass-produce of PSCs.

The relatively undoped (Sn^{4+}-free) and pinhole-free $CH_3NH_3SnI_3$ perovskite films and the near-single-crystalline $FASnI_3$ film have been fabricated.[22,45–47] If the background doping of $CH_3NH_3SnI_3$ can decrease to 10^{15} cm^{-3}, then L can reach to micrometers. With the advance in preparation technology, lead-free perovskite materials with low defect and longer diffusion can be achieved.

5. Conclusions

The effects of the carrier mobility and diffusion length on the PSC's performance are studied systematically with the device simulation. A similar parabolic relationship between the mobility of absorber and the efficiency for PSC to that for the organic solar cell is observed and there also exists an optimal mobility of the absorber. Diffusion length longer than 1 μm is also beneficial to the PSCs' performance when the absorber is thick and has high crystalline quality. The improved carrier mobility of the absorber and the HTM appropriately is favorable to the reduction of the recombination rate and the improvement of the carrier transportation, which can avoid the joint reduction of J_{sc}, and V_{oc} when the absorber layer thickness increases, and these can improve the cell's efficiency. The

doping of the carrier transport layer has a significant role in improving the cell performance. Finally, we obtain the J_{sc} of 34.21 mA/cm^2, V_{oc} of 0.942 V, FF of 84.97%, and PCE of 27.39% in our cell structure with an absorber thickness of 1200 nm, a high mobility of 12 cm^2/V·s, and long diffusion length of 2 μm. Using the hot casting method to realize high quality perovskite films may be a promising method to realize the high efficiency PSCs with thick absorber and high stability.

References

[1] Kim H S, Lee C R, Im J H, Lee K B, Moehl T, Marchioro A, Moon S J, Humphry-Baker R, Yum J H, Moser J E, Gratzel M and Park N G 2012 *Sci. Rep.* **2** 591

[2] Lee M M, Teuscher J, Miyasaka T, Murakami T N and Snaith H J 2012 *Science* **338** 643

[3] Jeon N J, Na H, Jung E H, Yang T Y , Lee Y G, Kim G, Shin H W , Seok S I, Lee J and Seo J 2018 *Nat. Energy* **3** 682

[4] Baikie T, Fang Y, Kadro J M, Schreyer M, Wei F, Mhaisalkar S G, Graetzel M and White T J 2013 *J. Mater. Chem. A* **1** 5628

[5] Phillips L J, Rashed A M, Treharne R E, Kay J, Yates P, Mitrovic I Z, Weerakkody A, Hall S and Durose K 2016 *Sol. Energy Mater. Sol. Cells* **147** 327

[6] Stranks S D, Eperon G E, Grancini G, Menelaou C, Alcocer M J, Leijtens T, Herz L M, Petrozza A and Snaith H J 2013 *Science* **342** 341

[7] Zhao Y, Nardes A M and Zhu K 2014 *J. Phys. Chem. Lett.* **5** 490

[8] Takahashi Y, Hasegawa H, Takahashi Y and Inabe T 2013 *J. Solid State Chem.* **205** 39

[9] Ponseca C S, Jr., Savenije T J, Abdellah M, Zheng K, Yartsev A, Pascher T, Harlang T, Chabera P, Pullerits T, Stepanov A, Wolf J P and Sundstrom V 2014 *J. Am. Chem. Soc.* **136** 5189

[10] Huang L, Sun X, Li C, Xu R, Xu J, Du Y, Wu Y, Ni J, Cai H, Li J, Hu Z and Zhang J 2016 *Sol. Energy Mater. Sol. Cells* **157** 1038

[11] Fu K, Zhou Q, Chen Y, Lu J and Yang S E 2015 *J. Opt.* **17** 105904

[12] Zhou Y and Gray-Weale A 2016 *Phys. Chem. Chem. Phys.* **18** 4476

[13] Da Y, Xuan Y and Li Q 2018 *Sol. Energy Mater. Sol. Cells* **174** 206

[14] Sheikh A D, Bera A, Haque M A, Rakhi R B, Gobbo S D, Alshareef H N and Wu T 2015 *Sol. Energy Mater. Sol. Cells* **137** 6

[15] Minemoto T and Murata M 2014 *J. Appl. Phys.* **116** 054505

[16] Kour N, Mehra R and Chandni 2018 *Chin. Phys. B* **27** 018801

[17] Adhikari K R, Gurung S, Bhattarai B K and Soucase B M 2016 *Phys. Status Solidi C* **13** 13

[18] Mandoc M M, Koster L J A and Blom P W M 2007 *Appl. Phys. Lett.* **90** 133504

[19] Deibel C, Wagenpfahl A and Dyakonov V 2008 *Phys. Status Solidi-Rapid Res. Lett.* **2** 175

[20] Ramírez O, Cabrera V and Reséndiz L M 2014 *Opt. Quantum Electron.* **46** 1291

[21] Shieh J T , Liu C H , Meng H F , Tseng S R , Chao Y C and Horng S F 2010 *J. Appl. Phys.* **107** 084503

[22] Du H J , Wang W C and Zhu J Z 2016 *Chin. Phys. B* **25** 108802

[23] Manser J S, Christians J A and Kamat P V 2016 *Chem. Rev.* **116** 12956

[24] He Y and Galli G 2017 *Chem. Mater.* **29** 682

[25] Jiang C S, Yang M, Zhou Y, To B, Nanayakkara S U, Luther J M, Zhou W, Berry J J, Lagemaat J, Padture N P, Zhu K and Al-Jassim M M 2015 *Nat. Commun.* **6** 8397

[26] Yang G, Ding B, Li Y, Huang S, Chu Q, Li C and Li C 2017 *J. Mater. Chem. A* **5** 6840

[27] Tan H, Jain A, Voznyy O, Lan X, Arquer F P G, Fan J Z, Bermudez R Q, Yuan M, Zhang B, Zhao Y, Fan F, Li P, Quan L N, Zhao Y, Lu Z H , Yang Z, Hoogl, S and Sargent E H 2017 *Science* **355** 722

[28] Shirayama M, Kadowaki H, Miyadera T, Sugita T, Tamakoshi M, Kato M, Fujiseki T, Murata D, Hara S, Murakami T N, Fujimoto S, Chikamatsu M and Fujiwara H 2016 *Phys. Rev. Appl.* **5** 014012

[29] Albrecht S, Saliba M, Correa-Baena J P , Jäger K, Korte L, Hagfeldt A, Grätzel M and Rech B 2016 *J. Opt.* **18** 064012

[30] Alnuaimi A, Almansouri I and Nayfeh A 2016 *J. Comput. Electron.* **15** 1110

[31] Abate A, Leijtens T, Pathak S, Teuscher J, Avolio R, Errico M E, Kirkpatrik J, Ball J M, Docampo P, McPherson I and Snaith H J 2013 *Phys. Chem. Chem. Phys.* **15** 2572

[32] Leijtens T, Lim J, Teuscher J, Park T and Snaith H J 2013 *Adv. Mater.* **25** 3227

[33] Toshniwal A, Jariwala A, Kheraj V, Opanasyuk A S and Panchal C J 2017 *J. Nano-Electron. Phys.* **9** 03038

[34] Edri E, Kirmayer S, Henning A, Mukhopadhyay S, Gartsman K, Rosenwaks Y, Hodes G and Cahen D 2014 *Nano Lett.* **14** 1000

[35] Liu X, Bu T, Li J, He J, Li T, Zhang J, Li W, Ku Z, Peng Y, Huang F, Cheng Y B and Zhong J 2018 *Nano Energy* **44** 34

[36] Zhang H, Shi J, Xu X, Zhu L, Luo Y, Li D and Meng Q 2016 *J. Mater. Chem. A* **4** 15383

[37] Liu D, Li S, Zhang P, Wang Y, Zhang R, Sarvari H, Wang F, Wu J, Wang Z and Chen Z D 2017 *Nano Energy* **31** 462

[38] Zhou Q, Jiao D, Fu K, Wu X, Chen Y, Lu J and Yang S E 2016 *Sol. Energy* **123** 51

[39] Iftiquar S M and Yi J 2018 *Mater. Sci. Semicond. Process* **79** 46

[40] Kavan L and Grätzel M 1995 *Electrochim. Acta* **40** 643

[41] Momblona C, Malinkiewicz O, Roldán-Carmona C, Soriano A, Gil-Escrig L, Bandiello E, Scheepers M, Edri E and Bolink H J 2014 *APL Mater.* **2** 081504

[42] Chen J, Zuo L, Zhang Y, Lian X, Fu W, Yan J, Li J, Wu G, Li C Z and Chen H 2018 *Adv. Energy Mater.* **8** 1800438

[43] Chiang C H and Wu C G 2016 *Nat. Photon.* **10** 196

[44] Dong Q, Fang Y, Shao Y, Mulligan P, Qiu J, Cao L and Huang J 2015 *Science* **347** 967

[45] Koh T M, Krishnamoorthy T, Yantara N, Shi C, Leong W L, Boix P P, Grimsdale A C, Mhaisalkar S G and Mathews N 2015 *J. Mater. Chem. A* **3** 14996

[46] Bansode U, Naphade R, Game O, Agarkar S and Ogale S 2015 *J. Phys. Chem. C* **119** 9177

[47] Shao S, Liu J, Portale G, Fang H H , Blake G R, ten Brink G H, Koster L J A and Loi M A 2018 *Adv. Energy Mater.* **8** 1702019